

# Drug characteristics of nanogels studied using Kinetic Monte Carlo simulations

Rakshit Kumar Jain, Sandip Samanta, and Prateek Kumar Jha\*

*Department of Chemical Engineering, IIT Roorkee, Roorkee, Uttarakhand 247667, India*

E-mail: pkjchfch@iitr.ac.in

Phone: +91-1332-284810

## Abstract

We theorize a new model for pressure-controlled stimuli-responsive nanogels to substantiate their role as effective drug carriers. Origin of pressure in the environment of the system can be attributed to the osmotic pressure of the solution in which the nanogel is immersed. Our proposed model, which has provisions for varying nanogel density and drug-polymer interactions does not, however, incorporate movements of the polymer matrix and changes in the shape of the gel. We use Kinetic Monte Carlo simulations to analyze the effects of initial state and the efficacy of varied nanogels as drug delivery devices. A comparative study between the effect of interaction force and the external pressure applied has also been done to ensure a complete study and enable calibration between their values. This method has been able to predict the tendency of the system to approach a steady state in a much faster and computationally efficient way, as opposed to the previous efforts in allied areas.

# Introduction

Nanogels are nano-sized interlocked polymer strands immersed in a liquid solvent which have gained importance in the recent years due to their versatile behavior. They have the unique capabilities of responding to external stimuli which have proven difficult to be modeled accurately. They have found their uses in many fields ranging from drug delivery<sup>12345</sup> and cleaning polluted rivers and streams to sensor technology and separation media.

Many studies have previously modeled their response to temperature<sup>678910</sup>, pH<sup>1011</sup>, electric fields as well as concentrations of ions in the polymer solution<sup>68</sup> via experimental, theoretical and computational methods<sup>12</sup>. Some studies also incorporate other forces and phenomena at play like erosion<sup>1314</sup>, convection due to the fluid in which it is placed as well as including nanogel swelling and shrinking in their theories<sup>12</sup>.

Most of the aforementioned studies look at the loading and release behavior of various macromolecules with respect to the polymer matrix under the effect of external stimulus. This serves as an important method to test the behavior of the model proposed as this is the feature which is used in most of the applications of the polymeric system.

Currently, most of the theoretical as well as computational methods are based on the Donnan Theory<sup>15</sup> or the Gibbs-Donnan effect of unequal distribution of charges around a semipermeable membrane, which is based on continuum mechanics. In this study we perform kinetic Monte Carlo (kMC) simulations on a spherical nanogel in a container, under the effect of an external pressure force. Kinetic Monte Carlo is a method recently developed which has extensive uses for ascertaining non-equilibrium properties of matter, as opposed to Monte Carlo methods, which are highly useful for equilibration of processes<sup>16</sup>. As opposed to the Donnan methodology, these simulations have the additional benefit of providing us a detailed look into particle fluctuations and small changes in the position as well as partial concentrations of the macromolecule being loaded or released. This also provides us the final structure of the drug delivery device obtained after loading as well as the structural properties of the device remaining after it releases the imbibed macromolecule.

Most simulation methodologies which need to look at detailed behavior of the migrating macromolecule do not consider polymer movement and assume that polymer relaxation time is too long<sup>12</sup>. This enables them to neglect the nanogel swelling or shrinking while the system changes. We will also apply the same assumption in our model, with the view that swelling could easily be incorporated in our model by integrating nanogel radius as a function of time, where we know the rate of swelling and shrinking of the nanogel.

Furthermore, the theories which incorporate polymeric structures of the nanogels, make inherent assumptions relating to the structure of the nanogel, assuming it to be either a perfect network or a network with well-defined imperfections<sup>789</sup>. Both these assumptions severely restrict the applicability of the results and are very difficult to be calculated experimentally. We, on the other hand, incorporate the distortions via means of density of the polymeric network in a spherical arrangement which can be used on any kind of model, be it a hollow shell<sup>1017</sup>, a core-shell nanogel, a gaussian density distribution or a nanogel of constant density.

There have been many simulation studies in the past, based on the Monte Carlo (MC)<sup>68</sup> as well as Molecular Dynamics (MD)<sup>18</sup> methods. They have yielded interesting results with limitations of the MD methods being that they are restricted to small networks with no relaxation in the polymer segments, since they have to operate at small length and time scales. MD simulations do have the benefit that they are able to provide a more detailed structure than our kMC methodology. MC methods are unable to capture release and loading simultaneously, as opposed to kMC simulations, which are able to do so, alongwith providing a more detailed structure than MC simulations.

We theorize a new model where we suggest the use of a pressure denoted by  $P$  to characterize any force which propels the drug molecules inside the nanogel. In most cases, this force will be a representation of the osmotic pressure generated due to the difference in concentration of drug molecules inside and outside the nanogel. In addition to that, it can be used to include any other external force (excluding, naturally, drug-polymer or drug-solvent

interactions) which affects the drug motility in the system. An example can be an external electrostatic field applied to charged systems to enhance the rate of drug loading or release.

In addition to the above mentioned pros, most of the parameters in our proposed model can easily be obtained by experimental means viz. the value of the external pressure on the nanogel, density of the matrix and the number of drug molecules present in the solution. A fitting parameter of our model is  $\epsilon_{n,d}$  which characterizes the interaction between the nanogel and the drug molecule, which is greater than zero if there is a repulsive force and is less than zero in the case of an attractive nanogel. This parameter ( $\epsilon_{n,d}$ ) can be altered to fit any given experimental data, or be used as a design parameter to obtain specifications for new nanogels.

## Models and methods

The loading and release mechanisms occur primarily due to some kind of impetus provided to the drug and/or the nanogel, as discussed in the previous section. In our case, we assume that the driving force behind the particle movement is pressure. This pressure can arise due to anything, from solvent's osmotic pressure to the force exerted by the electromagnetic or temperature field on the particles. Due to this, we introduce a potential energy contribution by the pressure force for each particle  $i$ , given by Eq. 1

$$U_{i,Pr}(r) = \frac{4}{3} \pi r^3 (P) \quad (1)$$

which has been derived from the standard thermodynamic expression  $E = P \cdot V$ , where  $P$  represents the external pressure applied, and  $V = (4/3)\pi r^3$ , gives the volume of the imaginary sphere of radius  $r$ , measuring the distance from the nanogel center to the particle center.

Next, to prevent the overlap of any two adjacent drug particles, we use the Lennard-Jones

potential as represented by Eq. 2

$$U_{ij,LJ}(r) = \begin{cases} 4\epsilon \left[ \left(\frac{\sigma}{r}\right)^{12} - \left(\frac{\sigma}{r}\right)^6 \right] + E_{cut} & r \leq r_{cut} \\ 0 & r > r_{cut} \end{cases} \quad (2)$$

which is valid for any pair of particles  $(i, j)$  with  $r_{cut} = 2^{1/6}\sigma$  being the cutoff distance.  $E_{cut}$  is the Lennard-Jones potential value at  $r = r_{cut}$  which prevents discontinuity at the termination point.

To make sure that particles do not overfill a region, we are also including the constraint over volume fractions given by Eq. 3

$$\rho_n + \rho_d \leq 1 \quad (3)$$

Here,  $\rho_n$  gives the volume fraction of the nanogel whereas  $\rho_d$  gives the volume fraction of the drug in the region being considered, meaning that for a nanogel with  $\rho_n = 0.5$ , the maximum allowed space for the drug molecules to enter is half of the total space available. Furthermore, in the cases where the inequality does not hold true, we add a penalty in the energy calculations to prevent it from accepting that move, which is given by

$$f_P(\rho_T) = 10^{12} \cdot \Theta(\rho_T - 1) \cdot \exp(\rho_T - 1) \quad (4)$$

where  $\rho_T(r) = \rho_d(r) + \rho_n(r)$  and  $\Theta$  represents the Heaviside function.

Interactions are also considered between nanogel and drug molecule, which only activate in the presence of both the nanogel and drug molecules. There are three kinds of 2-body interactions in the system, drug-polymer, polymer-polymer and drug-drug. Of these, since the polymer is treated as a continuum, it loses the energy contribution and the drug is assumed to be non-interacting with itself, leaving us with only the drug-polymer interactions,

which are given by Eq. 5

$$U_{i,int}(r) = \epsilon_{n,d} \rho_d \rho_n \quad (5a)$$

$$\text{where } \epsilon_{n,d} = \begin{cases} > 0 & \text{repulsive nanogel} \\ < 0 & \text{attractive nanogel} \end{cases} \quad (5b)$$

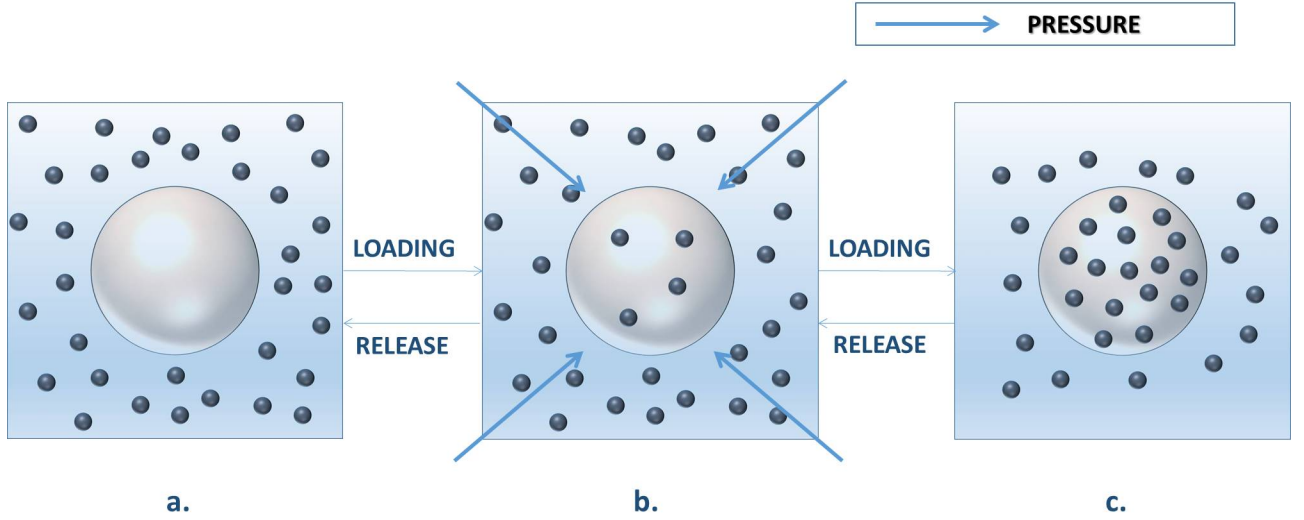


Figure 1: The grey sphere represents the nanogel and the smaller spheres give the particulate representations of the drug. We take  $\sigma = 1$  which is the diameter of the smaller sphere i.e. the drug, which is the length scale of our simulation. The arrows represent the direction of the pressure applied, which is radially inward

In our model, shown in Fig. 1, we simulate the nanogel matrix assuming that it is a sphere of constant radius, with the density taken as constant or varying with a gaussian function as and when needed. In the absence of nanogel, the particles are devoid of any hindrance from the density making the interaction forces between nanogel and the drug macromolecule are zero.

The loading and release behavior are studied in accordance with the image shown in Fig. 1. For the situation when we look at only the loading behavior, we begin from a state where there are no drug macromolecules loaded inside the nanogel, and the nanogel is

completely empty, as shown in Fig. 1a. Then, under the effect of a pressure force and all the other interactions defined above, the molecules move and any intermediary stage can be thought to be similar to Fig. 1b, with some molecules inside the nanogel and some molecules still outside, dissolved in the solution. At the steady state, we can assume that the nanogel is loaded to the maximum extent that it can be loaded, which is represented in Fig. 1c. As opposed to this, when we look at the release dynamics of a system, we need to start from a very compressed state, where the drug molecules are already loaded inside the nanogel, given by Fig. 1c. Then, as we will be exerting a lesser pressure value than the one which was used to generate the highly compressed state, the drug molecules are bound to get out of the nanogel. This will again lead to an intermediate state given by Fig. 1b. Now, on allowing the system to further release drug molecules, it can happen that there are very less drug molecules or no drug molecules left in the nanogel sphere. This is due to the fact that there is still the extra force of drug-nanogel interaction, given by Eq. 5a. This force can leave some drug molecules trapped in the nanogel matrix, even when we think that all the drug should be released. Finally, we are using periodic boundary conditions to simulate a larger system by just solving the Smoluchowski diffusion equation<sup>19,20</sup> for a single box.

In order to validate the above proposed equations using the model described, we use a kinetic Monte Carlo (kMC) simulation approach with the implementation already described in earlier works<sup>19,20</sup>. The kMC scheme is based on a definition of transition probabilities, which are taken to be identical to the works referenced as given by Eq. 6.

$$P(\mathbf{r}_{old} \rightarrow \mathbf{r}_{new}) = \frac{1}{1 + \exp(\beta\Delta E)} \quad (6)$$

Here, the symbols use their meanings as  $\mathbf{r}_{old}$  giving the initial position,  $\mathbf{r}_{new}$  giving the new position,  $\Delta E$  being the energy change during the move and  $\beta = 1/k_B T$ . Each step in our simulation is an attempt to move a particle by a fixed distance ( $a = 0.1\sigma$ ) but a random orientation<sup>19</sup> with a sweep being defined as one move being attempted for all the particles

present in the system. The time taken for this process is given by Eq. 7.

$$\Delta t = \frac{a^2}{12D} = \frac{1}{12} \left( \frac{a}{\sigma} \right)^2 \tau_0 \quad (7)$$

where  $D$  gives the diffusivity constant of the system and  $\tau_0 = \sigma^2/D$  gives the computational unit of time.

At each attempted move, we calculate the change in energy of the system using the equations 1, 2 and 5 under the effect of the constraints given by equations 3 and 6. Subsequently, we update the coordinates of the particle after every kMC step, the density of the whole system as required by equations 3 and 5a are updated after every kMC sweep, a needful approximation to keep a reasonable simulation time.

We also conduct a theoretical analysis to utilize one of the most prominent polymer thermodynamics studies, and use it to support our results. We define two phases, one consisting of the nanogel and the drug, denoted by I and another which has just the outer solvent and the drug, given by II. According to the lattice model for polymer thermodynamics, the potential energy at steady state can be given by

$$f(\phi_n^I, \phi_d^I) = \frac{k_B T}{v} [\phi_d^I \ln(\phi_d^I) + (1 - \phi_n^I - \phi_d^I) \ln(1 - \phi_n^I - \phi_d^I) + \chi_{dn} \phi_n^I \phi_d^I] \quad (8a)$$

$$f(\phi_d^{II}) = \frac{k_B T}{v} [\phi_d^{II} \ln(\phi_d^{II}) + (1 - \phi_d^{II}) \ln(1 - \phi_d^{II})] \quad (8b)$$

where  $v$  represents the molecular volume of the drug,  $\phi_d^I$  and  $\phi_d^{II}$  gives the drug volume fraction in phase I and II respectively.  $f()$  represents the free energy per unit volume for each of the defined phases of the system and  $\chi_{dn}$  represents the interaction constant between the drug and nanogel, used to calculate the potential gap needed for their interactive movement. Similarly for all the other denominations, they also follow the standard defined above. To check if the system has achieved steady state, we check the chemical potential equality, given



by

$$\mu_s^{II} = \mu_s^I \quad (9a)$$

$$\mu_d^{II} = \mu_d^I \quad (9b)$$

## Results and discussion

We perform simulations in a cubic box of size  $L = 72$  incorporating the periodic boundary conditions using the kinetic Monte Carlo simulation methodology described above. To prevent excessive crowding, we perform the simulations with  $N = 1728$  coarse grained drug molecules neglecting the polymer dynamics of the nanogel as we assume the polymer relaxation time to be high as well.

Before incorporating the nanogel into our system, it was necessary to observe the effects of external pressure on the behavior of drug molecules in order to justify the validity of our study. Hence, we carried out simulations at various external pressures in order to characterize the extent of drug entering the nanogel during loading and the exit of the molecules during release. To analyze the loading behavior, all the drug molecules were initially considered to be uniformly distributed over the simulation box, as there is no nanogel included in the system. Simulations were then performed for external pressures ranging from 0.0001 to a maximum value of 0.1, where we take 4 equally spaced step values for each order of magnitude. The steady state values of amount of drug loaded were noted from the block averaged plots for each external pressure applied. The extent of loading in each case has been evaluated as the number of drug molecules that are present in an imaginary sphere of radius 20. Similar methodology has been followed to examine the release behavior except that the initial state corresponds to the maximum loaded state as obtained from the steady state for pressure identical to 0.1. The simulation times around which averages were taken

are given in Table 1 for both the release and loading scenarios of the presented simulations.

Table 1: Simulation time around which averages are taken for the presented simulations

Pressure value	Loading time	Release time
0.0001	1245.7835	1499.94
0.00025	1249.95	1499.94
0.0005	1333.28	1833.26
0.00075	1416.61	1183.286
0.001	1291.65	1604.1025
0.0025	1208.285	1249.95
0.005	1083.29	1166.62
0.0075	1166.62	1166.62
0.01	1249.95	1166.62
0.025	1666.6	1666.6
0.05	1874.925	1791.595
0.075	1291.615	1333.28
0.1	1708.225	1249.95

As we can see from Fig. 2, at values of the applied external pressure greater than  $2.5 \times 10^{-3}$ , the error bars for the amount of drug inside our imaginary sphere for loading and release overlap. Therefore, we can say that here, the effect of initial state is not as apparent as it is in the earlier states. We observe that the initial state plays a deciding role at lower pressures, where we see a diverging characteristic in the amount of drug inside the sphere between loading and release (Fig. 2a). This behavior is observed due to the very less chemical potential generated by the initially-studied states, which have low pressure values. Due to the low chemical potential, the particles do not have enough gradient to move, and are suspended in a state close to the initial state during loading as well as release. Since the release state is a much compressed state, we expect to obtain discrepancy between them for less external pressures as seen here.

To further support the argument made in the previous section, we can look at Fig. 3, where we plot the time progress of the amount of drug molecule remaining in the imaginary sphere of radius  $r = 20$ . We can see that the number of drug molecules in the sphere increase when we are studying loading, whereas, they decrease for the case of release, before they achieve steady state.

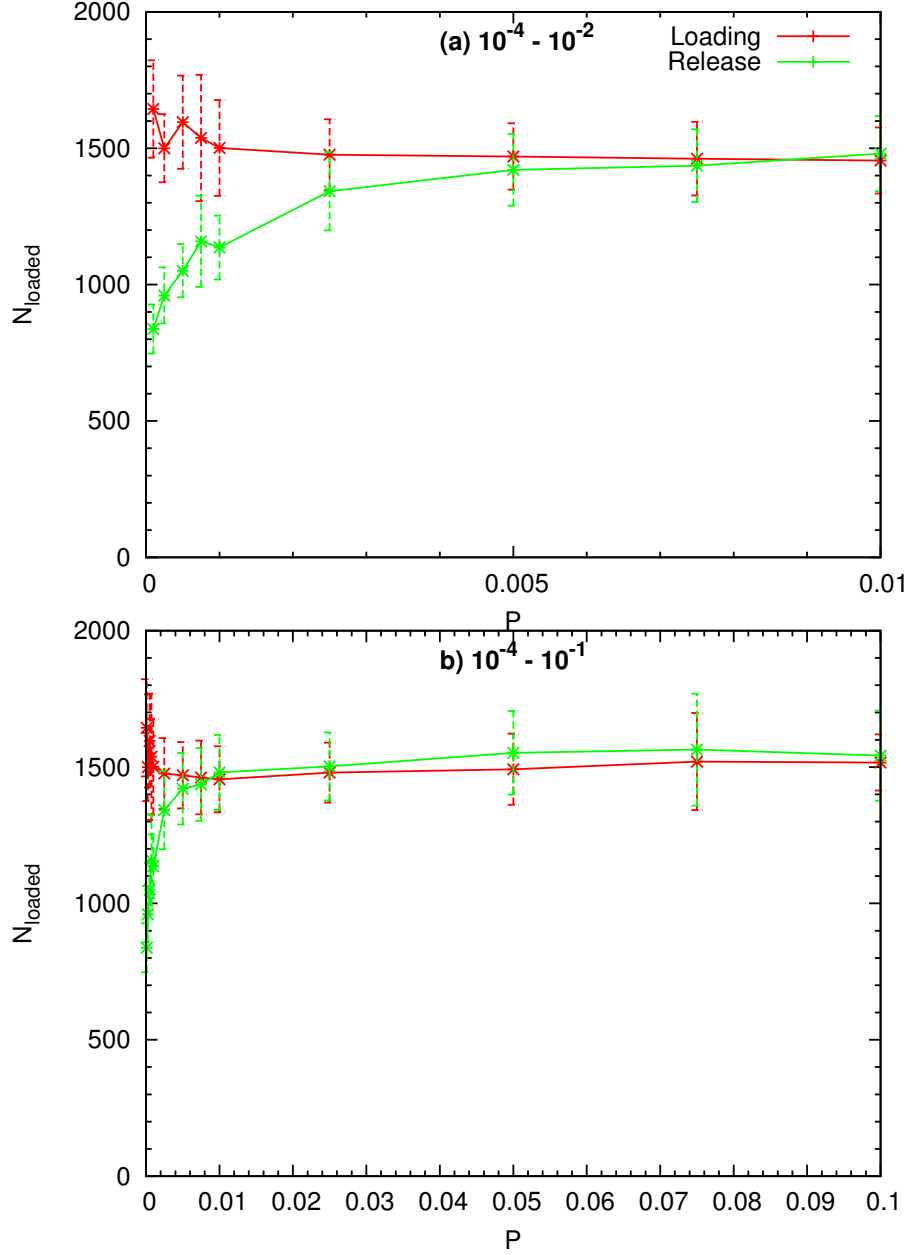


Figure 2: Plots representing the amount of drug loaded and released at various external pressures in the absence of nanogel

Thereafter, we include a nanogel that is a sphere with  $r_n = 10$  into our system, where  $r_n$  gives the radius of the nanogel. An attractive drug-polymer interaction potential with  $\epsilon_{n,d} = 10^{-3}$  was used to completely define the nanogel. Simulations were carried out for  $\rho_n = 0.5$  when we are including a nanogel of a uniform constant density. We limit our systems to

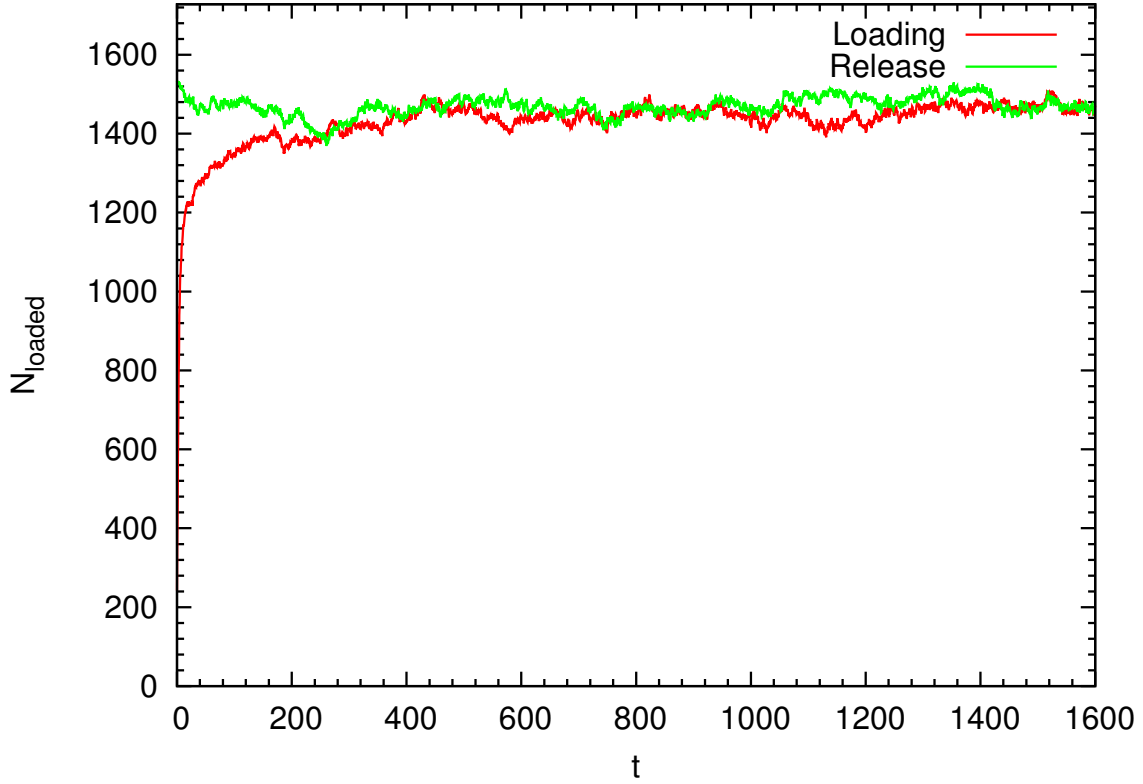


Figure 3: Plot representing the amount of drug loaded and released as a function of time for  $P = 0.01$  in the absence of nanogel

such a value as the best packing fraction of 0.74 is obtained in hexagonal close packing (hcp) or face centered cubic structures (fcc). Similar to the previous scenario where loading and release phenomena were separately observed, these simulations utilize only loading cycles. The loading pressure was maintained at a constant value of  $10^{-2}$ . In order to make our study more realistic, we have also looked at the nature of loading in a nanogel having the same radius and drug-polymer interaction as mentioned previously but where density varies as a Gaussian function given by Eq.10

$$\rho_{gauss}(r) = A \exp\left(\frac{-r^2}{c^2}\right) - B \quad \forall \quad r \leq r_n \quad (10)$$

To calculate the different parameters i.e.  $A$ ,  $B$  and  $c$ , we first assume two standard deviations on either side of the mean. This helps us to obtain  $\exp\left(\frac{-r_n^2}{c^2}\right) = 0.02$ , which gives us  $c = 5.0$ .

Since the nanogel density is expected to taper off at its surface, therefore, we further use

$$\rho_{gauss}(r) = A \exp\left(\frac{-r^2}{c^2}\right) - B = 0 \quad \text{at } r = 10 \quad (11)$$

which gives us  $B = 0.018315 \cdot A$ . We will further be comparing the loading behavior in the nanogel of a constant density and that with a gaussian variation. Therefore, we equate the amount of polymer contained in them, given by Eq. 12

$$\int_0^{10} \frac{4}{3} \pi r^3 \left( A \exp\left(\frac{-r^2}{c^2}\right) - B \right) dr = \int_0^{10} \frac{4}{3} \pi r^3 \rho_n dr \quad (12)$$

Using the previously calculated values of  $c$  and  $B$ , we get  $A = 147.54355$  when  $\rho_n = 0.5$ . The results displaying the comparisons for these two cases are demonstrated in Fig. 4.

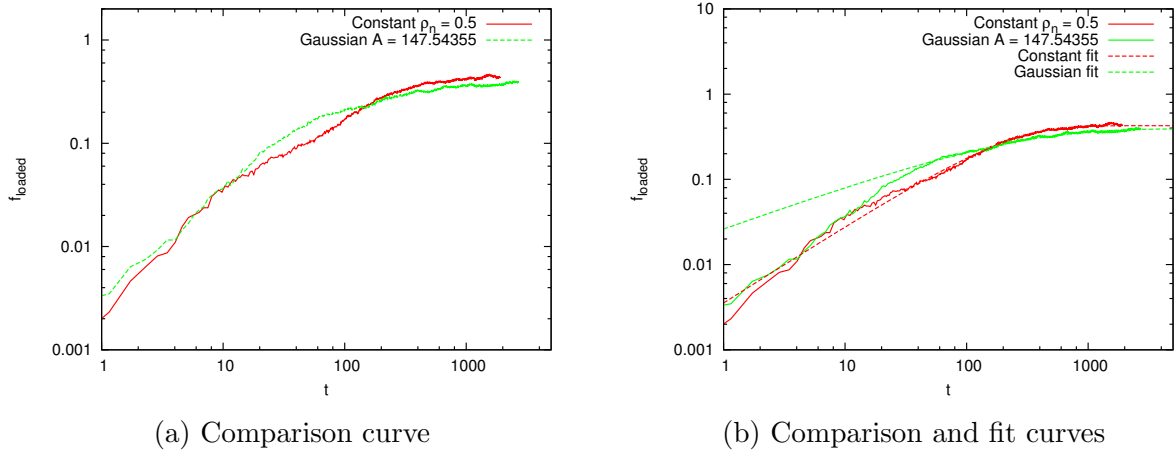


Figure 4: Plots representing the study between a constant density and a gaussian density nanogel

We now see in Fig. 4a that the final amount loaded is greater for a constant density nanogel as opposed to a gaussian density one, which is explained by the fact that even though the amount of polymer is same, the extremely filled core of the gaussian density sphere prevents the drug molecules to penetrate closer to the center. Another interesting feature is the existence of two zones, the first one where the amount being loaded is higher in the gaussian curve relative to the constant density one and the other one where this

behavior is reversed. A reasoning for this can be thought in terms of the tapering nature that is prevalent in a nanogel having gaussian density. Consequently, the portion of the sphere near  $r_n = 10$  will have very less polymeric material, and the drug loading rate is faster in that scenario. But, as time passes, the sphere gets filled up, and the drug molecules find it difficult to enter the nanogel. As opposed to this, for the constant density sphere, the amount of polymeric material is uniformly distributed, which offers uniform hindrance throughout and it overtakes after a certain amount of time.

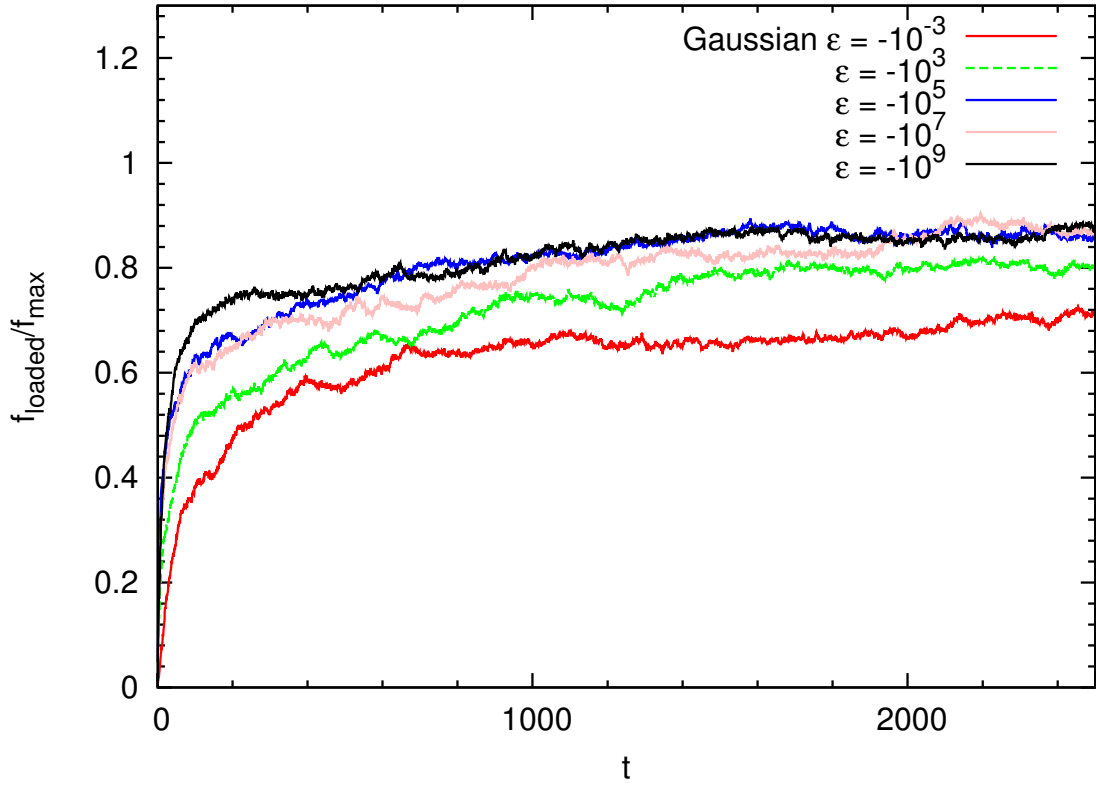
We further tried to fit the curves using a modified Weibull function given by

$$y = f_{max} \left( 1 - \exp \left( - \left( \frac{x}{a} \right)^b \right) \right) \quad (13)$$

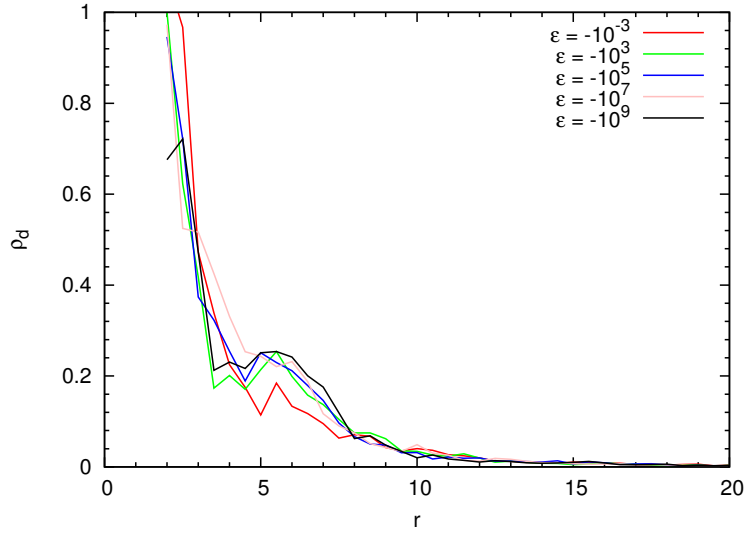
Here,  $f_{max}$  represents the maximum fraction of the drug loaded inside the nanogel in the respective case. As seen in Fig. 4b, we find that this function is able to fit our log comparison curves with remarkable accuracy. For the gaussian density nanogel, we get the fitting parameters as  $f_{max} = 0.392$ ,  $a = 176.738 \pm 0.7879$  and  $b = 0.516817 \pm 0.001656$  whereas for the constant density sphere we obtain  $f_{max} = 0.426$ ,  $a = 200.644 \pm 0.6997$  and  $b = 0.902361 \pm 0.004224$ .

For the sake of completeness, we now present our results on comparing the effect of pressure and the interaction between nanogel and drug molecule. We ran simulations keeping a constant loading pressure of 0.05 while varying the attractive force between the nanogel and drug using  $\epsilon_{n,d}$ , gradually from  $-10^{-3}$  to  $-10^9$  with the nanogel of a gaussian density profile detailed above. The results in Fig. 5a are plotted with the ratio between fraction drug loaded and the maximum drug loading seen, which is  $f_{max} = 0.55$  for  $\epsilon_{n,d} = -10^9$ . This is done so that the results are visible to a greater extent and the variations become more pronounced.

As visible from Fig. 5a, we see that however much we increase the value of  $\epsilon_{n,d}$ , there exists a maximum amount which can be loaded into the gaussian nanogel. Instinctively,



(a)



(b)

Figure 5: a.) Ratio of fractional amount loaded to the maximum loading for varying  $\epsilon_{n,p}$  in the case of a gaussian density nanogel b.) Volume fraction of loaded drugs as a function of the distance from the center at the steady state

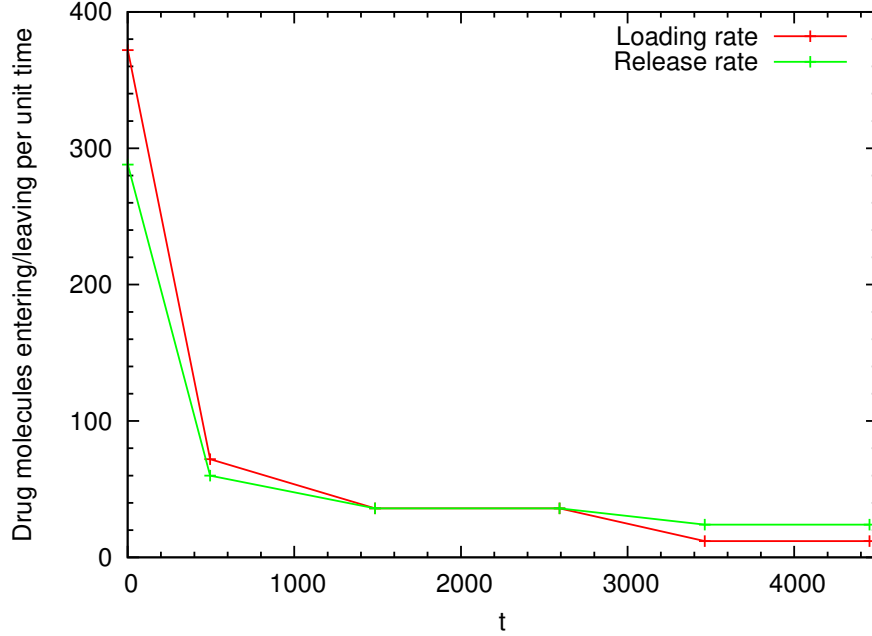


Figure 6: Plots representing the variation in loading rate and release rate for the shown cycle of  $\epsilon_{n,d} = -10^9$

it seems that the amount of drug being loaded into the nanogel should constantly increase if there is empty space inside the nanogel. This is opposed by two reasons. The first one is the fact that as the molecules move inside, they do so by ordering themselves in some form of arrangement, which means that there is a reduction in their entropy. This reduction in entropy is being compensated by the forces which are propelling the particles inside, namely the nanogel-drug attraction and the external pressure applied. As they move inside, it becomes more difficult for the forces to overcome the increasing entropic cost, and there will come a point when the particles would stop going in, leading to a saturation less than what is theoretically expected.

Another reason can be explained using Fig. 5b where we see a slight rise in the volume fraction of drug loaded near  $r = 6$ . A possible explanation for this can be that when we apply the pressure force, the particles are acted upon by a large force in a really short period of time, which would arrange them in a random manner, similar to how we fill grains in a container. As shaking the container releases free space inside the container, the drug



molecules arrange in such a way that the many empty spaces between them near  $r = 6$  is too small for other molecules to go through, creating a saturation level much before the nanogel is completely filled with drug molecules.

To confirm whether or not steady state is being achieved, we further calculate the loading and release rates at different time intervals for a specific  $\epsilon_{n,d}$ . We calculated the number of drug molecules entering and exiting the nanogel for a consecutive 1000 timesteps centered at one particular time, then averaging over them. The resultant graph is shown in Fig. 6. We observe that for the initial state, the loading rate is greater than the release rate, which is intuitive, as when there are no particles inside the nanogel, the pressure and the attractive force move the particles inside, but due to the random movement induced due to the kinetic Monte Carlo method, the particles have the probability of moving in all directions. Then, as time increases, the loading and release rates become equal as the loading rate is decreasing along with the release rate. Now, on further moving ahead in time, we see that the release rate becomes higher than the loading rate. This is only possible when the system is completely saturated with the drug molecules and the probability of exiting is much more than the probability of more molecules entering the gel, which means that steady state has been achieved.

Using the Lattice-Boltzmann polymer thermodynamics model defined in the previous section, we will try to gauge the closeness to steady state and validate our result as to whether there should exist a maximum limit to which particles can be loaded, even while we increase the  $\epsilon_{n,d}$  value. After doing the necessary calculations and equating the chemical potentials, we get the final equations of the form

$$\phi_d^I(1 - \phi_d^I - \phi_n^I)^{-\phi_n^I} + c(1 - \phi_d^I - \phi_n^I)^{-\phi_n^I+1} - c = 0 \quad (14a)$$

$$\text{with } c = e^{-\chi_{dn}\phi_n^I} \quad (14b)$$

Representing the above equations in a graphical format, we can get Fig. 7. This plot clearly

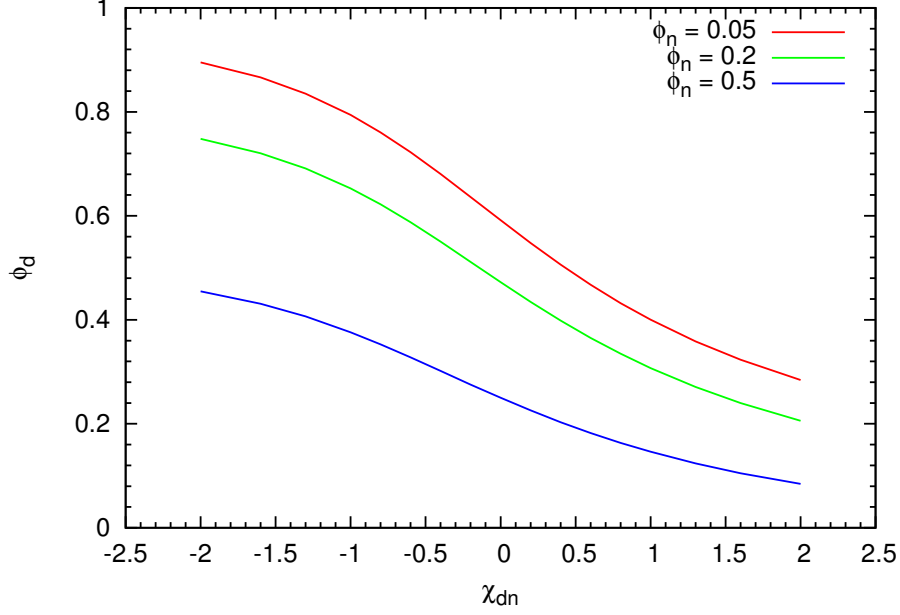


Figure 7: Plot representing the theoretical calculation of volume fraction of drug loaded at various interaction forces between the nanogel and drug, at varied nanogel volume fraction

shows that for a higher nanogel volume fraction, the amount of drug loaded is significantly less. Furthermore, on increasing  $\chi_{dn}$ , we find that the amount of drug loaded decreases. In polymer thermodynamics,  $\epsilon$  and  $\chi$  usually follow a linear relationship with each other, thus making them similar parameters. When we decrease  $\epsilon_{n,d}$ , we find that the amount of drug loaded increases, as seen in Fig. 5a. Similarly, when we decrease  $\chi_{dn}$ , we see that there is an increase in the amount of drug loaded. This proves that our supposition has yielded correct results. The graphs in Fig. 7 also tend to a constant value, which support our hypotheses as well as the results obtained via simulations that there exists a maximum value to which the nanogel can be loaded, irrespective of the interaction forces between the nanogel and the drug.

## Conclusion

We have proposed a new theory which is able to capture the loading and release behavior in the case of nanogels very effectively and further used kinetic Monte Carlo simulations to

verify the same, by neglecting the polymer relaxation dynamics and treating the nanogel as a fixed sphere of constant radius. Variations like incorporating a nanogel of variable size as well as including the effect of solvent on the size of the nanogel have not been included, which can form the basis of future studies.

Our results regarding the verification of particle movement in the absence of the nanogel are remarkable in the sense that they have not been replicated before by using various methods like Brownian Dynamics or Dissipative Particle Dynamics. The two phases of loading seen during comparison between the nanogel of a constant density and that of a gaussian density are also interesting as they also have a sound theoretical basis. The existence of a maximum amount of drug molecules which can be loaded inside a nanogel when studying the effect of  $\epsilon_{n,d}$ , is also supported by the theory of polymer thermodynamics. We have also analysed the loading and release rates in the system to qualify the closeness to steady state.

The experimental verification of our study has yet to be done, and if successful, it can be a major step in understanding the behavior of gels. This can provide an efficient controlling mechanism for stimuli-responsive gels, as with the help of pressure we are emulating the osmotic pressure exerted by the solvent on the nanogel.

## References

- (1) Ariga, K.; Kawakami, K.; Hill, J. P. *Expert Opinion on Drug Delivery* **2013**, *10*, 1465–1469, PMID: 23834331.
- (2) DAGANI, R. *Chemical & Engineering News Archive* **1997**, *75*, 26–37.
- (3) Doyle, F. J.; Dorski, C.; Harting, J. E.; Peppas, N. A. Control and modeling of drug delivery devices for the treatment of diabetes. American Control Conference, Proceedings of the 1995. 1995; pp 776–780 vol.1.

- (4) Kabanov, A.; Vinogradov, S. *Angewandte Chemie International Edition* **2009**, *48*, 5418–5429.
- (5) others,, et al. **2013**,
- (6) Quesada-Prez, M.; Ahualli, S.; Martn-Molina, A. *The Journal of Chemical Physics* **2014**, *141*, 124903.
- (7) Quesada-Prez, M.; Ahualli, S.; Martn-Molina, A. *Journal of Polymer Science Part B: Polymer Physics* **2014**, *52*, 1403–1411.
- (8) Quesada-Perez, M.; Martin-Molina, A. *Soft Matter* **2013**, *9*, 7086–7094.
- (9) Maldonado-Valderrama, J.; del Castillo-Santaella, T.; Adroher-Benitez, I.; Moncho-Jorda, A.; Martin-Molina, A. *Soft Matter* **2017**, *13*, 230–238.
- (10) Xing, Z.; Wang, C.; Yan, J.; Zhang, L.; Li, L.; Zha, L. *Soft Matter* **2011**, *7*, 7992–7997.
- (11) Manga, R. D.; Jha, P. K. *Journal of Pharmaceutical Sciences* **2017**, *106*, 629 – 638.
- (12) Escobedo, F. A.; de Pablo, J. J. *Physics Reports* **1999**, *318*, 85 – 112.
- (13) Siepmann, J.; Gpferich, A. *Advanced Drug Delivery Reviews* **2001**, *48*, 229 – 247, Mathematical Modeling of Controlled Drug Delivery.
- (14) Sackett, C. K.; Narasimhan, B. *International Journal of Pharmaceutics* **2011**, *418*, 104 – 114, Mathematical modeling of drug delivery systems:.
- (15) Jha, P. K.; Zwanikken, J. W.; Olvera de la Cruz, M. *Soft Matter* **2012**, *8*, 9519–9522.
- (16) Zhang, R.; Jha, P. K.; Olvera de la Cruz, M. *Soft Matter* **2013**, *9*, 5042–5051.
- (17) Chen, Y.; Zheng, X.; Qian, H.; Mao, Z.; Ding, D.; Jiang, X. *ACS Applied Materials & Interfaces* **2010**, *2*, 3532–3538, PMID: 21080640.
- (18) Everaers, R.; Kremer, K. *Phys. Rev. E* **1996**, *53*, R37–R40.

- (19) Jha, P. K.; Kuzovkov, V.; Grzybowski, B. A.; Olvera de la Cruz, M. *Soft Matter* **2012**, *8*, 227–234.
- (20) Jha, P. K.; Kuzovkov, V.; Olvera de la Cruz, M. *ACS Macro Letters* **2012**, *1*, 1393–1397.

## Graphical TOC Entry

Some journals require a graphical entry for the Table of Contents. This should be laid out "print ready" so that the sizing of the text is correct. Inside the `tocentry` environment, the font used is Helvetica 8 pt, as required by *Journal of the American Chemical Society*. The surrounding frame is 9 cm by 3.5 cm, which is the maximum permitted for *Journal of the American Chemical Society* graphical table of content entries. The box will not resize if the content is too big: instead it will overflow the edge of the box. This box and the associated title will always be printed on a separate page at the end of the document.